Chromophore Structure in Bacteriorhodopsin's O_{640} Photointermediate†

Steven O. Smith, Johannes A. Pardoen, Patrick P. J. Mulder, Bo Curry, Johan Lugtenburg, and Richard Mathies*

ABSTRACT: Resonance Raman spectra of the O_{640} photointermediate of bacteriorhodopsin have been obtained with a dual-beam, time-resolved technique. A flowing purple membrane suspension is first illuminated with a 514-nm laser beam to initiate photocycling. Raman scattering from O_{640} is excited 3–6 ms "downstream" with a probe beam at 752 nm. Raman spectra of the O_{640} intermediate have been obtained from native bacteriorhodopsin in H_2O and D_2O, as well as from bacteriorhodopsin regenerated with 15-deuterio- and 12,14-dideuterioretinals. O_{640} has a Schiff base line at 1628 cm^{-1}, which shifts to 1589 cm^{-1} in D_2O, demonstrating that the Schiff base is protonated. The pattern of vibrations in the 1100–1400-cm^{-1} fingerprint region of the O_{640} Raman spectrum is very similar to that observed in BR_{568}, which contains an all-trans protonated Schiff base chromophore. Furthermore, the frequency and intensity changes observed in the Raman spectra of 15-deuterio- and 12,14-dideuterio-O_{640} correspond closely with the deuteration-induced changes displayed by BR_{568}. However, the changes observed upon deuteration of the chromophore in BR_{548}, the 13-cis component of dark-adapted bacteriorhodopsin, are very different from those observed in O_{640}. These comparisons demonstrate that the retinal chromophore in O_{640} has an all-trans configuration. Therefore, the M_{412} to O_{640} conversion involves 13-cis to all-trans chromophore isomerization and protonation of the retinal–lysine Schiff base. In addition, the O_{640} spectrum exhibits strong hydrogen out-of-plane wagging vibrations that are not seen in BR_{568}. This indicates that the 13-trans chromophore in O_{640} is *conformationally* distorted.

Bacteriorhodopsin (BR),[1] the retinal–protein complex in the purple membrane of *Halobacterium halobium*, functions as a light-driven proton pump (Stoeckenius & Bogomolni, 1982; Birge, 1981). Light absorption drives the light-adapted form of the pigment BR_{568} through a cyclic photochemical reaction (Figure 1), which results in the transport of protons across the bacterial cell membrane. Resonance Raman and chemical extraction studies have demonstrated that the retinal chromophore in BR_{568} has an all-trans configuration and is attached to the protein through a protonated retinal–lysine Schiff base linkage (Braiman & Mathies, 1980; Tsuda et al., 1980; Aton et al., 1977; Pettei et al., 1977; Lewis et al., 1974). Photolysis of BR_{568} forms the red-absorbing intermediate K_{610}, which thermally decays through the intermediates L_{550}, M_{412}, and O_{640}, returning to BR_{568} in ~10 ms. Since the blue-absorbing M_{412} intermediate contains an unprotonated 13-cis Schiff base chromophore (Braiman & Mathies, 1980; Tsuda et al., 1980; Aton et al., 1977; Pettei et al., 1977; Lewis et al., 1974), the conversion of M_{412} back to BR_{568} must involve both reisomerization of the retinal chromophore and reprotonation of the Schiff base. Formation of O_{640}, the principal intermediate in the $M_{412} \rightarrow BR_{568}$ conversion, is kinetically associated with the uptake of protons by the cell membrane (Lozier et al., 1975), and its subsequent decay completes the BR photocycle. To determine the molecular mechanism for "resetting" this light-activated proton pump, we have used resonance Raman spectroscopy as an in situ probe of the chromophore structure in O_{640} [for a review on Raman spectroscopy see Mathies (1979)].

Raman spectra of the O_{640} intermediate were obtained by recirculating light-adapted bacteriorhodopsin through a glass capillary that is irradiated with a strong "pump" laser beam at 514 nm to initiate the BR photocycle. Raman scattering is then excited with a 752-nm "probe" laser beam spatially displaced from the pump beam. The pump–probe separation (3–6 ms) is adjusted to produce the maximum concentration of O_{640} in the flowing stream as the sample crosses the probe beam. The far-red probe excitation provides favorable enhancement of O_{640} scattering and also reduces interference from O_{640} fluorescence.

To determine the chromophore structure in O_{640}, we employ an "isotopic fingerprint" method that has previously been used to establish the configuration of the chromophore in BR_{568}, M_{412}, and K_{625} (Braiman & Mathies, 1980, 1982). Bacterioopsin samples from a retinal-deficient mutant of *H. halobium* are regenerated with 15-deuterio- and 12,14-dideuterioretinal. The deuterium shifts observed in the 1100–1400-cm^{-1} fingerprint regions of the Raman spectra of these derivatives are characteristically different for pigments containing 13-cis and all-trans chromophores. We use light-adapted bacteriorhodopsin (BR_{568}) and the 13-cis component of dark-adapted bacteriorhodopsin (BR_{548}) as "model compounds" containing protonated all-trans and 13-cis chromophores, respectively. Comparison of the deuteration-induced changes observed in their Raman spectra with those observed in O_{640} permits the assignment of the chromophore configuration in O_{640}. In addition, Raman spectra of O_{640} obtained with purple membrane suspended in D_2O establish the protonation state of the Schiff base nitrogen.

Materials and Methods

Retinal Derivatives. Crystalline *all-trans*-retinal (Eastman Kodak) was shown to be >98% pure by high-performance liquid chromatography and was used without further purification. *all-trans*-15-Deuterioretinal was prepared by $LiAlD_4$ reduction of *all-trans*-retinoic acid (Eastman Kodak), followed by MnO_2 oxidation (Braiman & Mathies, 1980). *all-trans*-12,14-Dideuterioretinal was prepared from β-ionone. The

† From the Chemistry Department, University of California, Berkeley, California 94720 (S.O.S., B.C., and R.M.), and the Department of Chemistry, Leiden University, 2300 RA Leiden, The Netherlands (J.A.P., P.P.J.M., and J.L.). *Received April 12, 1983.* This work was supported by grants from the NSF (CHE 81-16042) and the NIH (EY 02051). R.M. is an NIH Research Career Development Awardee (EY 00219). Research in Leiden was supported by grants from SON and ZWO.

[1] Abbreviations: BR, bacteriorhodopsin; PSB, retinal-protonated Schiff base; HOOP, hydrogen out-of-plane; 15D, 15-deuterioretinal; 12,14-D_2, 12,14-dideuterioretinal; 15H, unlabeled retinal; 12,14-H_2, unlabeled retinal; SDS, sodium dodecyl sulfate; Hepes, 4-(2-hydroxyethyl)-1-piperazineethanesulfonic acid.

0006-2960/83/0422-6141$01.50/0

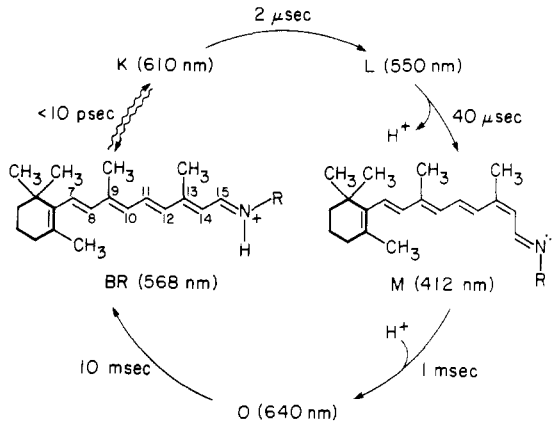

FIGURE 1: Proton-pumping photocycle of light-adapted bacteriorhodopsin (Lozier et al., 1975). Absorption maxima and room temperature decay times are indicated. BR_{568} contains an all-trans protonated Schiff base chromophore, while M_{412} contains an unprotonated 13-cis Schiff base. In the dark, BR_{568} slowly converts to dark-adapted bacteriorhodopsin, BR_{560}, which contains a 40/60 mixture of all-trans and 13-cis protonated Schiff base chromophores (denoted BR_{568} and BR_{548}, respectively).

C_{18}-acetylenic alcohol was first synthesized by coupling β-ionone with propargylmagnesium bromide, followed by acetylation with acetic anhydride. Base-catalyzed elimination of the resulting acetate group at C_9 with sodium amide and 1,5-diazabicyclo[4.3.0]non-5-ene, followed by reaction with *n*-butyllithium and acetaldehyde at −60 °C, yielded the C_{18}-acetylenic alcohol. $LiAlD_4$ reduction of the triple bond and quenching with H_2O, followed by MnO_2 oxidation of the alcohol, formed the 12-deuterio C_{18}-ketone. Incorporation of the second deuteron at C_{14} was accomplished by reaction of the 12-deuterio C_{18}-ketone with deuterated acetonitrile and *n*-butyllithium. The product was worked up in three steps, involving (1) acetylation with acetic anhydride, (2) elimination of the acetate group with 1,5-diazabicyclo[4.3.0]non-5-ene, and (3) reduction of the cyano group with diisobutylaluminum hydride, to form the 12,14-dideuterioretinal aldehyde. ^1H NMR of *all-trans*-12,14-dideuterioretinal exhibits the expected loss of the H_{12} and H_{14} doublets at 6.37 and 5.97 ppm, and collapse of the H_{11} quartet to a doublet at 7.13 ppm and the aldehyde doublet to a singlet at 10.10 ppm. The deuterated retinal derivatives were shown to be 95% isotopically and >98% isomerically pure by mass spectrometry, NMR, and high-performance liquid chromatography (J. A. Pardoen, P. P. J. Mulder, and J. Lugtenburg, unpublished results).

White Membrane. A retinal-deficient mutant of *H. halobium* (strain JW5) was obtained from H. J. Weber, University of California, San Francisco. Cells were cultured and lysed according to published procedures (Oesterhelt & Stoeckenius, 1974; Braiman & Mathies, 1980). White membrane was obtained by two to four differential centrifugations at 25000*g* for 90 min in a Beckman JA-21 centrifuge (JA-20 rotor), followed by density gradient centrifugation (25–45% sucrose) at 80000*g* for 10–15 h in a Beckman L8-70 ultracentrifuge at 10 °C (SW-27 rotor). Electrophoresis of the resulting preparation on SDS–polyacrylamide gels (10% polyacrylamide, 0.1% sodium dodecyl sulfate) demonstrated that white membrane consists of a single protein, bacterioopsin ($M_r \simeq 26000$).

White membrane was regenerated under dim red light by using 2 mM solutions of *all-trans*-retinal in ethanol. First, a small aliquot of white membrane was removed, and regeneration was followed by monitoring the absorption increase at 568 nm and the disappearance of the free retinal absorption band at 380 nm. Retinal was added to regenerate only 90–95% of the bacterioopsin, in order to avoid excess retinal in the samples used for Raman spectroscopy. The absorption spectrum after regeneration was similar to that of native purple membrane with the exception of a small band at 410 nm, which gave a 410 nm/568 nm absorbance ratio of 0.31 vs. 0.23 for native purple membrane. This absorption has been ascribed to contaminating respiratory pigments (Mukohata et al., 1981). The nonregenerated protein is estimated to be <20% of the total protein on the basis of the relative absorbance at 280 and 568 nm. White membrane has no visible circular dichroism but characteristic bands at 600, 530, and 315 nm appear after regeneration, indicating that the protein exists as trimers in the regenerated white membrane.

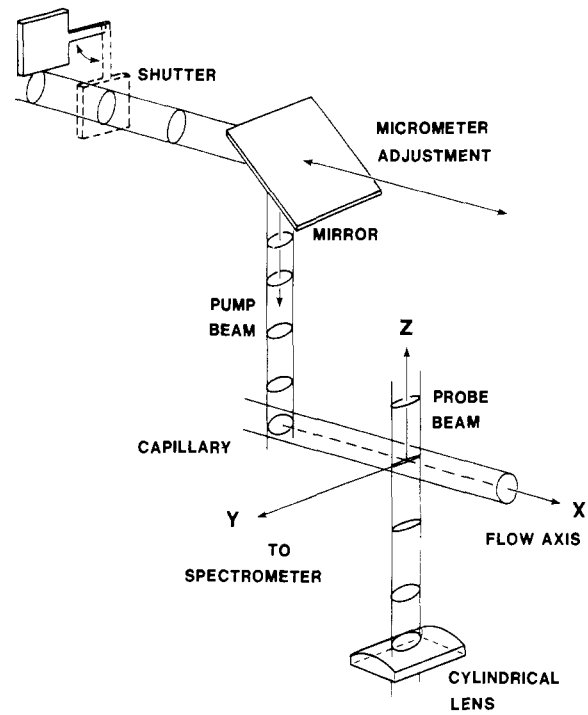

FIGURE 2: Millisecond time-resolved Raman apparatus. The time delay (0.2–20 ms) is set by displacing the pump beam upstream from the probe. The computer-controlled shutter makes it possible to obtain probe-only and pump-and-probe spectra for each monochromator setting.

Raman spectra of BR_{568}, BR_{548}, and M_{412} obtained from regenerated white membrane were identical with Raman spectra obtained from native purple membrane. Raman spectra of nonregenerated white membrane displayed no Raman lines under the conditions used. The use of regenerated white membrane is advantageous because it does not contain carotenoid contamination, or the retinal oxime which is produced in the alternative bleaching procedure for native purple membrane (Braiman & Mathies, 1980).

Raman Spectroscopy. Raman spectra were obtained on a Spex 1401 double monochromator with a Spex 1419 illuminator and photon counting detection (PAR 1105/1120). The monochromator was stepped in 2-cm^{-1} increments, and the spectral resolution was 4 cm^{-1}. Vibrational frequencies are accurate to ±2 cm^{-1}. Digital data were averaged, smoothed (three-point sliding average), corrected for detector sensitivity, and fluorescence backgrounds (simulated by a quartic polynomial) were subtracted with a PDP 11/23 computer. Excitation at 647 and 752 nm was obtained from a Spectra-Physics 171-01 krypton ion laser, and excitation at 514 nm was obtained from a Spectra-Physics 165 argon ion laser.

O_{640} Spectra. The dual-beam flow apparatus used to obtain Raman spectra of O_{640} is shown in Figure 2. Bacteriorhodopsin was circulated at a velocity of 200–300 cm/s

through a long glass capillary (diameter of 1.4 mm). The sample reservoir was maintained at 40 °C and illuminated with a 100-W incandescent light to keep the purple membrane light adapted. Raising the temperature to 40 °C served to increase the proportion of O_{640} formed (Maentele et al., 1981; Lozier et al., 1975). The sample (25–50 mL) was buffered in distilled water at pH 7 with 10 mM Hepes and had an optical density of 2/cm at 570 nm.

Raman spectra of O_{640} were obtained with a 200-mW, 752-nm probe laser beam spatially displaced from a 500-mW, 514-nm pump laser beam. The time separation between the pump and probe beams was controlled by translating the pump beam along the capillary. The useful time range of this apparatus is 0.2–20 ms. The optimal spatial separation (3–6 ms) was determined by monitoring the laser-induced fluorescence from O_{640}. The rise time ($t_{1/2}$) of O_{640} fluorescence in H_2O at 40 °C was ~1.6 ms and the decay time was ~5.0 ms, in agreement with time-resolved absorption results (Lozier et al., 1975). The use of far-red probe excitation together with the 3–6-ms time delay results in pump-and-probe spectra that contain contributions only from O_{640} and unphotolyzed BR_{568}. Probe-only spectra of pure BR_{568} were obtained by blocking the photolysis beam. A shutter system (Uniblitz 26L) was interfaced to the PDP 11/23 computer and programmed to take alternate pump-and-probe and probe-only data points at each wavelength setting of the monochromator. The dwell times were 2–4 s per data point, and typical spectra represented the average of ~30 scans. Difference spectra were generated by computer subtraction of the probe-only (BR_{568}) spectra from the pump-and-probe (BR_{568} + O_{640}) spectra. The correct subtraction parameter was determined by complete subtraction of the prominent 1526-cm^{-1} line of BR_{568} and the absence of inverted peaks, which would result from oversubtraction.

The probability that the retinal chromophore will photoreact during passage through the laser beam is given by the photoalteration parameter F (Mathies et al., 1976). Estimating the extinction coefficient at 752 nm for O_{640} as 5000 M^{-1} cm^{-1} (Lozier et al., 1975) and assuming a quantum yield of unity, we adjusted the probe laser power (200 mW cylindrically focused) to keep $F \leq 0.1$. The 500-mW pump beam was spherically focused to irradiate the entire diameter of the flow capillary, thereby maximizing the conversion of BR_{568} to O_{640} ($F = 1.3$).

BR_{548} Spectra. In the absence of light, bacteriorhodopsin converts to a dark-adapted state (BR_{560}) containing a mixture of all-trans and 13-cis protonated Schiff base chromophores (Sperling et al., 1977). Raman spectra of BR_{560} were obtained with >100 mL of purple membrane solution circulated at 28 °C through the capillary. The low-photoalteration probe excitation (20 mW) at 647 nm was cylindrically focused. It is generally assumed that BR_{568} has the same spectrum as the all-trans component of BR_{560} (Marcus & Lewis, 1978; Stockburger et al., 1979; Aton et al., 1979; Terner et al., 1979b). Raman spectra of the 13-cis component of dark-adapted bacteriorhodopsin, BR_{548}, were obtained by subtraction of a light-adapted BR_{568} spectrum from the spectrum of BR_{560}. Typical spectra of BR_{560} and BR_{568} represent the average of ~10 scans using 2-cm^{-1} steps and 1–2-s dwell times.

Results

Figure 3 presents Raman spectra of purple membrane at 40 °C taken in the absence (Figure 3A) and presence (Figure 3B) of a spatially separated pump beam at 514 nm. Subtraction of the probe-only (BR_{568}) spectrum from the pump-and-probe (BR_{568} + O_{640}) spectrum yields the Raman spectrum of the O_{640} intermediate (Figure 3C). Distinctive lines

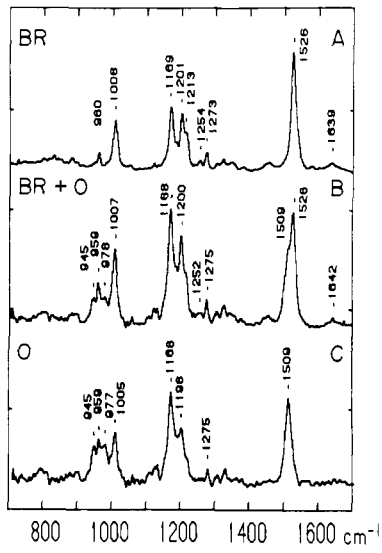

FIGURE 3: Resonance Raman spectra of purple membrane taken with a 200-mW, 752-nm probe beam in the absence (A) and presence (B) of a temporally separated (4 ms) 500-mW, 514-nm pump beam. (C) Raman spectrum of O_{640} obtained by subtracting 60% of (A) from (B).

in the O_{640} spectrum are an ethylenic stretching vibration at 1509 cm^{-1}, fingerprint lines at 1168, 1198, and 1275 cm^{-1}, and lines in the hydrogen out-of-plane region at 945, 959, and 977 cm^{-1}. Raman spectra of O_{640} previously obtained by Terner et al. (1979a) using 550-nm single-beam excitation are significantly different from the green-pump, red-probe spectra presented here. In particular, they observed an ethylenic line at 1520 cm^{-1}, major fingerprint lines at 1172 and 1187 cm^{-1}, and no strong lines in the 945–977-cm^{-1} range. To determine whether relative intensity changes result from the difference in probe wavelength, we have also obtained Raman spectra of O_{640} exciting at 603 nm on the blue edge of the O_{640} fluorescence band. These spectra are very similar to our 752-nm probe spectra. In the earlier experiments the use of green-probe excitation results in strong resonance enhancement of Raman scattering from unphotolyzed BR_{568} and from L_{550}, making it difficult to obtain a pure spectrum of O_{640} by subtraction. Furthermore, the stationary sample arrangement employed by Terner et al. (1979a) in combination with high-photoalteration green-probe excitation could have produced additional photoproducts of BR_{568}, L_{550}, and O_{640}.

Figure 4 presents Raman spectra of purple membrane at 40 °C in D_2O. Suspending purple membrane in D_2O results in an increase in the concentration of the O_{640} intermediate (Maentele et al., 1981), so that the pump-and-probe spectrum (Figure 4B) contains a larger contribution from the O_{640} component. A pure spectrum of O_{640} in D_2O is presented in Figure 4C. Comparison of Figures 3 and 4 shows that the O_{640} fingerprint is only slightly perturbed by suspension in D_2O. The most noticeable change is the apparent shift of the 977-cm^{-1} line to 957 cm^{-1} in D_2O.

Figure 5 presents higher signal-to-noise spectra of the Schiff base region of O_{640} in H_2O and D_2O. The shift of the 1628-cm^{-1} line observed in H_2O (Figure 5A) to 1589 cm^{-1} in D_2O (Figure 5B) is good evidence that O_{640} has a protonated Schiff base. The observed frequency of the C=N stretch, however, is unusually low compared with BR_{568}. Deuteration at C_{15} shifts the C=N stretch of O_{640} to 1607 cm^{-1} (data not shown).

The fingerprint vibrations from 1100 to 1400 cm^{-1} can be described as mixtures of C–C stretches and CCH rocks, and they are sensitive to the configuration of the retinal chain. Both all-trans and 13-cis aldehydes and Schiff bases in solution

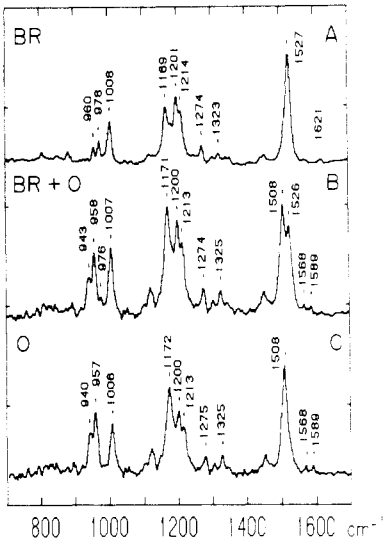

FIGURE 4: Resonance Raman spectra of purple membrane suspended in D_2O taken with a 752-nm probe beam in the absence (A) and presence (B) of a temporally separated (5 ms) 514-nm pump beam. (C) Raman spectrum of O_{640} in D_2O obtained by subtracting 30% of (A) from (B).

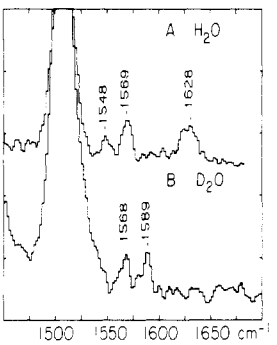

FIGURE 5: Schiff base region of the O_{640} Raman spectra in H_2O (A) and D_2O (B). High signal-to-noise spectra were obtained by averaging 120 scans for H_2O and 42 scans for D_2O under the same conditions used in Figures 3 and 4.

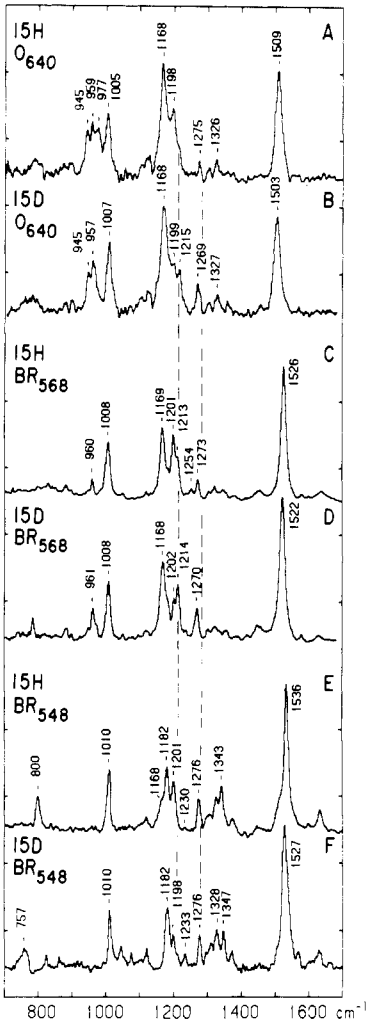

FIGURE 6: Comparison of native and 15-deuterio regenerated O_{640}, BR_{568}, and BR_{548} Raman spectra: (A) native 15H O_{640} spectrum; (B) O_{640} regenerated with 15-deuterioretinal; (C) native 15H BR_{568} spectrum (752-nm probe); (D) BR_{568} regenerated with 15-deuterioretinal; (E) native 15H BR_{548} spectrum (647-nm probe); (F) BR_{548} regenerated with 15-deuterioretinal.

exhibit fingerprint vibrations that are characteristic of the double-bond configuration (Mathies et al., 1977). When these isomers are bound in bacteriorhodopsin, it is often more difficult to distinguish between them because the protein-induced changes are comparable in magnitude to the differences in frequencies and intensities between the all-trans and 13-cis isomers. We have observed, however, that deuteration at specific positions near the C_{13}=C_{14} bond allows these isomers to be distinguished even in the presence of protein perturbations (Braiman & Mathies, 1980, 1982). Thus, to determine the configuration of the chromophore in O_{640}, we compare the spectra of native *and isotopically labeled* O_{640} with all-trans and 13-cis model compounds.

Figure 6 presents Raman spectra of O_{640} obtained with native bacteriorhodopsin (15H) and bacterioopsin regenerated with 15-deuterioretinal (15D). These spectra are compared with spectra of 15H and 15D BR_{568} and BR_{548}. First, it should be noted that the native O_{640} spectrum is very similar to that of BR_{568}, particularly with respect to the frequencies and relative intensities of the 1169-, 1201-, and 1213-cm^{-1} fingerprint lines. On the other hand, the BR_{548} spectrum is significantly different from that of O_{640} or BR_{568}, because BR_{548} has only a weak shoulder at 1168 cm^{-1}, an intense line at 1182 cm^{-1}, and no shoulder at ~1215 cm^{-1}. Furthermore, C_{15}-deuteration of O_{640} (Figure 6B) results in an apparent decrease of intensity in the 1198-cm^{-1} line and an intensity increase at 1215 and 1269 cm^{-1}. The spectral changes occurring upon deuteration of BR_{568} exhibit a similar pattern. In the 15D BR_{568} spectrum (Figure 6D), a loss of intensity is observed in the 1201-cm^{-1} line, the 1254-cm^{-1} line disappears, and an increase of intensity results at 1214 and 1270 cm^{-1}. 15H and 15D spectra of BR_{548} are shown in parts E and F of Figure 6 for comparison. In the 13-cis model compound deuteration results in a loss of intensity at 1168 cm^{-1}, decreased intensity at 1201 cm^{-1}, and increased intensity at 1233 cm^{-1}. The relative intensity of the 1276-cm^{-1} line, however, does not change. The changes observed for O_{640}, then, are more analogous to those observed in BR_{568}. The close similarity of the native BR_{568} and O_{640} spectra in conjunction with the 15D isotopic derivative comparison suggests that O_{640} contains all-trans chromophore. If this is correct, O_{640} spectra obtained with other derivatives of retinal deuterated near the C_{13}=C_{14} bond should also show changes characteristic of an all-trans chromophore.

In Figure 7, Raman spectra of O_{640} obtained with bacterioopsin regenerated with 12,14-dideuterioretinal (12,14-D_2) are compared with corresponding spectra of BR_{568} and BR_{548}. These spectra were obtained in D_2O in order to increase the amount of O_{640} in the sample. Deuteration at C_{12} and C_{14} results in a number of distinctive changes in the fingerprint region of O_{640} (Figure 7A,B). The intense line at 1172 cm^{-1}

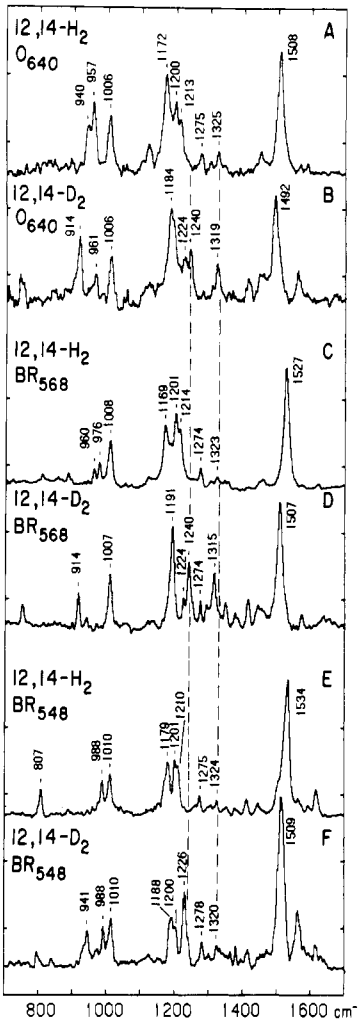

FIGURE 7: Comparison of native and 12,14-dideuterio regenerated O_{640}, BR_{568}, and BR_{548} Raman spectra in D_2O: (A) native 12,14-H_2 O_{640} spectrum; (B) O_{640} regenerated with 12,14-dideuterioretinal; (C) native 12,14-H_2 BR_{568} spectrum in D_2O (752-nm probe); (D) BR_{568} regenerated with 12,14-D_2 retinal; (E) native 12,14-H_2 BR_{548} spectrum in D_2O (647-nm probe); (F) BR_{548} regenerated with 12,14-D_2 retinal.

in unsubstituted O_{640} has shifted to 1184 cm^{-1} in the 12,14-D_2 derivative. There are also new lines appearing at 1224, 1240, and 1319 cm^{-1}. In addition, an intense line has shifted down to 914 cm^{-1}. The pattern of spectral changes in BR_{568} is very similar to the pattern observed in O_{640}. The intense fingerprint line at 1169 cm^{-1} (Figure 7C) shifts to 1191 cm^{-1} (Figure 7D), and new lines appear at 1224, 1240, and 1315 cm^{-1}. A new line also appears at 914 cm^{-1} in the low wavenumber region. The deuteration-induced changes in BR_{548}, however, are quite different. In 12,14-D_2 BR_{548}, intensity shifts from 1201 and 1210 cm^{-1} to a new line at 1226 cm^{-1} (Figure 7F). Also, an intense new line appears at 941 cm^{-1}, which should be contrasted with the 914-cm^{-1} line in 12,14-D_2 BR_{568} and O_{640}. The close similarity of the deuteration-induced changes in O_{640} and in BR_{568} argues strongly that O_{640} contains an *all-trans*-retinal chromophore.

Discussion

Isotopic comparisons similar to those presented here for O_{640} have been used to show that M_{412} and K_{625} contain 13-cis chromophores, while BR_{568} contains an all-trans chromophore (Braiman & Mathies, 1980, 1982). The deuteration-induced changes in these spectra can now be interpreted more quantitatively on the basis of recent progress in the assignment of the vibrational spectra of retinal and BR_{568} (Curry et al., 1982, 1984; Braiman, 1983). While a complete vibrational analysis of BR and its photointermediates is not yet available, it is useful to discuss the present data in detail so that the rationale behind the isotopic fingerprint method will be clear. Also, a careful examination of the O_{640} spectra provides more detailed information on the chromophore configuration, conformation, and state of protonation.

Fingerprint Vibrations. BR_{568}, which contains an all-trans protonated Schiff base (PSB), serves as a model pigment in our discussion of vibrational assignments. We have used a series of BR_{568} isotopic derivatives to show that the C_{10}–C_{11} stretch is localized in the normal mode at 1169 cm^{-1} while the C_{14}–C_{15} and C_8–C_9 stretches are found at 1201 and 1213 cm^{-1}, respectively. The C_{12}–C_{13} stretch is much more delocalized, having its largest contributions to normal modes at 1169 and 1254 cm^{-1} (S. Smith, J. A. Pardoen, J. Lugtenburg, and R. Mathies, unpublished results). With these assignments the spectral changes induced by C_{15}-deuteration can be understood. C_{15}-Deuteration removes the coupling of the $C_{15}H$ rock with the C_{14}–C_{15} stretch so this stretch would be expected to shift up in frequency. The loss of intensity at 1201 cm^{-1} and the increased intensity at 1214 and 1270 cm^{-1} can then be attributed to this upshift of C_{14}–C_{15} stretch character. The 1254-cm^{-1} band is more difficult to characterize because it is weak and contains both C_{12}–C_{13} stretch and $C_{15}H$ rock character. In the 15-deuterio derivative the 1254-cm^{-1} band disappears when the $C_{15}H$ rock component shifts down to ~974 cm^{-1}. Thus the "C_{12}–C_{13} stretch" either loses intensity or shifts into near degeneracy with the 1270-cm^{-1} line. A similar pattern of spectral changes is exhibited by the retinal model compounds upon C_{15}-deuteration (Braiman & Mathies, 1980). In the all-trans PSB spectra, the 1197-cm^{-1} line shifts to 1202 cm^{-1}, and the 1239-cm^{-1} line disappears. We attribute these changes to the upshift of the C_{14}–C_{15} stretch and the redistribution of C_{12}–C_{13} stretch character. The *pattern* of frequency and intensity shifts is thus the same in BR_{568} and in the all-trans PSB of retinal, reflecting similar coupling between the $C_{15}H$ rock and the C–C stretches in all-trans chromophores.

Comparison with the spectral changes in O_{640} shows a number of similarities. Deuteration at C_{15} leads to a shift of intensity from 1198 to 1215 cm^{-1} and an increase of intensity in the line at 1269 cm^{-1} (Figure 6A,B). The close similarity of these frequency and intensity changes argues that 15D substitution causes a similar upshift of the C_{14}–C_{15} stretch and redistribution of C_{12}–C_{13} stretch character. Unfortunately, a line corresponding to the 1254-cm^{-1} BR_{568} line cannot be identified in the O_{640} spectrum. It should be noted, however, that the 1254-cm^{-1} line in BR_{568} is weak with 752-nm excitation and a corresponding line in O_{640} may have escaped detection.

The pattern of spectral changes induced by deuteration is expected to be sensitive to the frequency of the C_{14}–C_{15} stretch and its coupling with the other single-bond stretches. Isomerization would be expected to alter both of these factors and lead to different spectral changes for the 13-cis isomers. We have used the 13-cis component of dark-adapted bacteriorhodopsin, BR_{548}, as our 13-cis model compound. Isotopic derivatives of BR_{548} indicate that the C_{14}–C_{15} stretch is localized at 1168 cm^{-1}, the C_{10}–C_{11} stretch is at 1182 cm^{-1}, and the C_8–C_9 stretch is at 1201 cm^{-1}. The C_{12}–C_{13} stretch is again quite delocalized, with its largest components at 1230 and 1168 cm^{-1} (S. Smith, J. A. Pardoen, J. Lugtenburg, and R. Mathies, unpublished results). The major difference between BR_{548} and BR_{568} is the lower frequency of the normal

modes involving the C_{14}–C_{15} and C_{12}–C_{13} stretches. This is consistent with the prediction by Curry et al. (1984) that single-bond stretches adjacent to a cis bend should be lowered in frequency. In analogy with the all-trans isomer, the increase of intensity at 1233 cm^{-1} when C_{15} is deuterated can be attributed to an upshift of C_{14}–C_{15} stretch character from 1168 cm^{-1} when coupling of the $C_{15}H$ rock with the C_{14}–C_{15} stretch is eliminated. A band appears near 1230 cm^{-1} upon deuteration at C_{15} in K_{625}, in M_{412}, and in the protonated and unprotonated Schiff bases of 13-*cis*-retinal (Braiman & Mathies, 1980, 1982) and is therefore very characteristic of 13-cis chromophores. Thus, the fact that 15D substitution does *not* induce a line near 1230 cm^{-1} in O_{640} is evidence against a 13-cis configuration.

It is also possible to give a more detailed description of the spectral changes induced by 12,14-dideuterio substitution in O_{640}, BR_{568}, and BR_{548}. Deuteration at C_{12} and C_{14} should particularly affect the frequency of the C_{12}–C_{13} stretch. An upshift of the C_{12}–C_{13} stretch would be expected to result from C_{12}-deuteration because coupling between the $C_{12}H$ rock and the C_{12}–C_{13} stretch is eliminated. We have recently shown that the $C_{14}H$ rock is also strongly coupled with the C_{12}–C_{13} stretch but only weakly coupled with the C_{14}–C_{15} stretch (Curry et al., 1984). Thus, 12,14-D_2 substitution should cause an upshift of the C_{12}–C_{13} stretch as well as an upshift of other skeletal stretches with which the C_{12}–C_{13} stretch is coupled. The simplest interpretation of the 12,14-D_2 BR_{568} spectrum (Figure 7D) is that the 1240-cm^{-1} line represents the C_{12}–C_{13} stretch, which also contributes significantly to the 1315-cm^{-1} line, accounting for its increased Raman intensity. The C_{10}–C_{11} stretch (which is somewhat coupled with the C_{12}–C_{13} stretch) would then have shifted up into near degeneracy with the C_{14}–C_{15} stretch at 1191 cm^{-1}. The 10-cm^{-1} drop of the C_{14}–C_{15} stretch upon C_{14}-deuteration is consistent with its behavior in 14-deuterio- and 12,14-dideuterio-*all-trans*-retinal (Curry et al., 1984). Also, the expected weak coupling of the 1214-cm^{-1} C_8–C_9 stretch with the $C_{12}H$ rock results in a 10-cm^{-1} upshift of this vibration to 1224 cm^{-1} in 12,14-D_2 BR_{568}.

The changes observed in the Raman spectrum of 12,14-D_2 O_{640} are remarkably similar to those observed upon deuteration of BR_{568} (Figure 7B). New fingerprint lines appear at 1224, 1240, and 1319 cm^{-1}, and the intense 1172-cm^{-1} line shifts to 1184 cm^{-1} when C_{12} and C_{14} are deuterated. The 1172-cm^{-1} line has been assigned to the C_{10}–C_{11} stretch on the basis of an 8-cm^{-1} downshift in 10-^{13}C-labeled O_{640} (S. Smith, J. A. Pardoen, J. Lugtenburg, and R. Mathies, unpublished results). By analogy with BR_{568}, we attribute the appearance of the 1240- and 1319- cm^{-1} lines in 12,14-D_2 O_{640} to the upshift of C_{12}–C_{13} stretch character. The very similar pattern of frequency shifts observed in O_{640} and BR_{568} reflects similar vibrational coupling near the C_{13}=C_{14} bond and argues that the chromophores have the same configuration.

Deuteration of BR_{548} at C_{12} and C_{14} shifts fingerprint intensity into a band at 1226 cm^{-1}, and no new lines with significant intensity are observed above this frequency. One possible explanation is that the 1226-cm^{-1} line results from the upshifted C_{12}–C_{13} stretch. The 1226-cm^{-1} line may also contain significant contributions from the C_{14}–C_{15} and C_8–C_9 stretches, but this is difficult to quantitate. A similar shift of fingerprint intensity to 1227 cm^{-1} is observed upon 12,14-deuteration in K_{625}, which also contains a 13-cis chromophore (Braiman, 1983). Normal mode calculations on BR_{548} based on these observed spectral shifts and assignments, as well as further studies using deuterated retinal derivatives, should permit a more detailed characterization of the 1226-cm^{-1} line.

Table I: Deuterated In-Plane Rocking Vibrations of 12D, 14D, and 12,14-D_2 Derivatives[a]

	$C_{12}D + C_{14}D$	$C_{12}D - C_{14}D$	$C_{12}D$	$C_{14}D$
all-trans-retinal	901 (908)	1003 (1006)	972 (967)	959 (961)
13-*cis*-retinal	936 (939)	1044 (1036)	1040 (1036)	957 (955)
BR_{568}	914		981	975
O_{640}	914			
BR_{548}	941			

[a] All frequencies are in wavenumbers. The *all-trans*- and 13-*cis*-retinal data are from Curry (1983) and Curry et al. (1982, 1984). The 12D and 14D BR_{568} data are from Braiman (1983). Numbers in parentheses are the calculated frequencies.

In-Plane Rocking Vibrations. Vibrational analysis of *all-trans*- and 13-*cis*-retinal has demonstrated that the frequencies of the in-plane rocking vibrations of the C_{12} and C_{14} hydrogens are sensitive to the configuration about the C_{13}=C_{14} bond (Curry et al., 1984). The characteristic dependence of these frequencies on configuration is most apparent when the C_{12} and C_{14} positions are deuterated, since their rocking vibrations are then shifted into the 900–1050-cm^{-1} range, where they are relatively isolated from C–C stretches and other CCH rocks. The deuterated rocks in 12-deuterio- and 14-deuterio-*all-trans*-retinal lie at similar frequencies (972 and 959 cm^{-1}, respectively) but split apart to form out-of-phase and in-phase combinations at 1003 and 901 cm^{-1} when both are deuterated (see Table I). The all-trans chromophore of BR_{568} conforms to this pattern. The isolated $C_{12}D$ and $C_{14}D$ rocks of monodeuterated BR_{568} derivatives appear at 981 and 975 cm^{-1}, respectively (Braiman, 1983), while in the 12,14-D_2 derivative the intense in-phase rock combination appears at 914 cm^{-1}. The 13-cm^{-1} higher frequency of the in-phase combination in 12,14-D_2 BR_{568} (914 cm^{-1}) compared to its frequency in 12,14-dideuterio-*all-trans*-retinal (901 cm^{-1}) is consistent with the higher frequencies of the isolated $C_{12}D$ and $C_{14}D$ rocks in the monodeuterated BR_{568} species.

In 13-*cis*-retinal, steric repulsion between the C_{12} and C_{15} hydrogens as well as increased coupling with the C_{13}-methyl stretch causes the $C_{12}D$ rock to appear at a higher frequency than in the all-trans isomer (Curry et al., 1984). The $C_{12}D$ rock of 12-deuterio-13-*cis*-retinal appears at 1040 cm^{-1}, and the $C_{12}D + C_{14}D$ combination in the 12,14-D_2 derivative is also elevated in frequency (936 cm^{-1}). The 35-cm^{-1} increase of the latter frequency in the 13-cis isomer is an excellent indicator of the configuration about C_{13}=C_{14} because of the intensity of this line and its unambiguous assignment.

The steric interaction and altered vibrational coupling responsible for the increased $C_{12}D$ rock frequency of the 13-cis aldehyde are conserved in the 13-cis pigments. For example, in 12,14-D_2 BR_{548} the in-phase $C_{12}D + C_{14}D$ combination is observed at 941 cm^{-1} (Figure 7F), compared to 914 cm^{-1} in BR_{568}. The 12,14-D_2 derivatives of M_{412} and K_{625} exhibit lines at 943 and 941 cm^{-1}, respectively (Braiman, 1983). Since M_{412} contains an unprotonated 13-cis Schiff base chromophore and K_{625} contains a protonated 13-cis Schiff base chromophore (Braiman & Mathies, 1980, 1982), a line near 940 cm^{-1} in pigments containing 12,14-dideuterioretinal argues for a 13-cis configuration regardless of the nature of the end group.

In 12,14-D_2 O_{640} a line is observed at 914 cm^{-1}, which we assign as the low-frequency (in-phase) combination of the $C_{12}D$ and $C_{14}D$ rocks in analogy with the 914-cm^{-1} line in BR_{568}. Furthermore, no lines are observed in the 940-cm^{-1} frequency region characteristic of the $C_{12}D + C_{14}D$ combination in 13-cis chromophores. However, we must consider the possibility that intensity from the isolated $C_{11}H$ out-of-plane wag contributes

to the band at 914 cm^{-1} (Curry et al., 1982). In BR_{568} and BR_{548} as well as *all-trans*- and 13-*cis*-retinal, the hydrogen out-of-plane (HOOP) modes have very little Raman intensity, so the uncoupled $C_{11}H$ wag would not be expected to appear with intensity in the 12,14-D_2 derivatives. Thus, in these molecules an intense line in the 900–950-cm^{-1} region can unambiguously be assigned to the deuterated in-plane rock combination. In O_{640} the $C_{11}H$ and $C_{12}H$ out-of-plane wags may be responsible for one of the HOOP modes near 960 cm^{-1} (see below), and deuteration at C_{12} would be expected to leave the isolated $C_{11}H$ wag in the 900–925-cm^{-1} region with observable intensity (Curry et al., 1982). However, regardless of the position of the $C_{11}H$ out-of-plane wag, the low-frequency $C_{12}D + C_{14}D$ rock combination should also appear with intensity in the low wavenumber region of the Raman spectrum as it does in 12,14-D_2 BR_{568}, BR_{548}, M_{412}, K_{625}, *all-trans*-retinal, and 13-*cis*-retinal. Assuming that the $C_{12}D + C_{14}D$ rocking vibration also has significant intensity in O_{640}, we must assign it at 914 cm^{-1} since no other strong lines are observed in the 900–945-cm^{-1} region. Therefore, the observation of an intense 914-cm^{-1} line in 12,14-D_2 O_{640} supports the conclusion that O_{640} has an all-trans configuration. These results also demonstrate that the deuterated rock frequencies provide a valuable diagnostic tool for determining the chromophore configuration in retinal pigments.

Hydrogen Out-of-Plane Vibrations. The strong lines in the Raman spectrum of O_{640} at 977, 959, and 945 cm^{-1} can be assigned to hydrogen out-of-plane wagging vibrations on the basis of our isotopic data. The line at 977 cm^{-1}, which disappears in the 15D spectrum of O_{640} (Figure 6B) and shifts to 957 cm^{-1} in D_2O (Figure 4C), can be assigned to the C_{15} HOOP. The frequency drop of the $C_{15}H$ wag in D_2O is attributed to reduced coupling with the ND wag. The lines at 945 and 959 cm^{-1} most likely result from the $HC_7{=}C_8H$ and $HC_{11}{=}C_{12}H$ "A_u" HOOP's on the basis of their close correspondence to the group frequencies for such A_u vibrations (Potts & Nyquist, 1959; Curry et al., 1982). Except for the $C_{15}H$ wag, which we have already assigned, no wags other than the two A_u HOOP modes are expected in this region. Intense HOOP modes have been observed in K_{625} (Braiman & Mathies, 1982) and in the primary visual photoproduct, bathorhodopsin (Eyring et al., 1982), both of which are the direct products of photoisomerization. It has been shown that ground-state conformational distortion is the most likely cause of this unusual Raman intensity (Eyring et al., 1980; Warshel & Barboy, 1982). The presence of intense HOOP modes in O_{640} indicates that the all-trans chromophore in O_{640} is also conformationally distorted. Thus there is a strong correlation between HOOP Raman intensity (i.e., conformational distortion) and the production of a *configurationally* isomerized product. In both K_{625} and O_{640}, the same HOOP vibrations appear to be enhanced (the $C_{15}H$ HOOP and the $HC_7{=}C_8H$ and $HC_{11}{=}C_{12}H$ A_u HOOP modes), and they appear at remarkably similar frequencies in the K_{625} spectrum (973, 957, and 945 cm^{-1}) and in the O_{640} spectrum (977, 959, and 945 cm^{-1}) (Smith et al., 1983). This indicates similar distortions in the retinal chromophore, although the isomerization mechanisms that form K_{625} and O_{640} are very different. K_{625} is formed from an excited-state trans → cis *photo*isomerization, whereas O_{640} is formed from a ground-state *protein-catalyzed* cis → trans isomerization. In O_{640} the twists appear to be delocalized, occurring near C_{15}, $C_{11}{=}C_{12}$, and $C_7{=}C_8$. This suggests that during the formation of O_{640} a conformational change occurs which is delocalized throughout the chromophore. Viewed in isolation, this would be unexpected for an isomerization about the $C_{13}{=}C_{14}$ bond, but it is consistent with the hypothesis of charge perturbation near the ionone ring (Nakanishi et al., 1980), which might stabilize more delocalized structural changes.

Protonation State of O_{640}. Our Raman spectra of purple membrane suspended in D_2O, as well as those of Terner et al. (1979a), demonstrate that the Schiff base nitrogen in O_{640} is protonated. The red-shifted absorption maximum of O_{640} is consistent with this conclusion. The Schiff base frequency of O_{640} at 1628 cm^{-1} is lower than that observed in other protonated Schiff base compounds. For comparison, the C=NH stretch is at 1640 cm^{-1} for BR_{568} and at 1662 cm^{-1} for the all-trans PSB (Braiman & Mathies, 1980). The unusually low C=N frequency in O_{640} is consistent with a highly delocalized ground-state electronic structure, which would lower the effective C=N stretching force constant. Also, the drop of the O_{640} Schiff base line in D_2O (39 cm^{-1}) is significantly greater than that of BR_{568} (20 cm^{-1}) or the all-trans PSB (25 cm^{-1}). These large deuteration-induced shifts indicate that there is a stronger interaction between the NH rock and the C=N stretch in O_{640} than in other protonated Schiff bases (Curry et al., 1982; Aton et al., 1980). The $C_{15}H$ rock in O_{640} is also strongly coupled with the C=N stretch, as evidenced by the 21-cm^{-1} drop of the C=N stretch in 15D O_{640} vs. a 10-cm^{-1} drop in 15D BR_{568} and a 14-cm^{-1} drop in the 15D all-trans PSB.

The coupling between the hydrogen rocks and the C=N stretch can be described by a balance of kinetic interactions and through-space repulsive interactions between the hydrogens and the opposing carbon or nitrogen atoms. Increasing the C=N bond length tends to *increase* the net coupling between the rocks and the stretch by *decreasing* the through-space interaction. This suggests that the C=N stretch is more fully conjugated with the delocalized π system in O_{640} than in BR_{568}, which might be caused by displacement of the Schiff base from its counterion. A similar mechanism may be operative in the K_{625} intermediate (Rothschild & Marrero, 1982). The low C=N stretching frequency in K_{625}, as well as the transfer of infrared intensity to ~1580 cm^{-1} in ND K_{625} and to 1600 cm^{-1} in 15D K_{625} (Rothschild & Marrero, 1982; Bagley et al., 1982), is remarkably similar to the Schiff base frequencies observed in our O_{640} Raman spectra.

Conclusions

The vibrational assignments derived from these isotopic data and the assignments of Braiman (1983) provide a more quantitative interpretation of the vibrational spectra of bacteriorhodopsin and its intermediates. Comparison of the spectral changes in isotopic derivatives of O_{640} with changes in BR_{568} and BR_{548} demonstrates that the chromophore in O_{640} is an all-trans protonated Schiff base. In addition, O_{640} exhibits intense HOOP vibrations, which indicate that the trans chromophore has a distorted *conformation* about single bonds which must then relax as BR_{568} is formed.

It will now be important to determine whether the formation of O_{640} from M_{412} proceeds through a single step involving both isomerization and protonation or whether these structural changes proceed serially through the N_{520} intermediate. It will also be interesting to examine the branching of the photocycle at the M_{412} stage in high ionic strength solutions (Nagle et al., 1982). Further time-resolved Raman studies should help to resolve these questions.

Acknowledgments

We thank H. J. Weber for providing the retinal-deficient strain of *H. halobium*. We are also grateful to M. Braiman

and A. Myers for critical comments on the vibrational assignments.

References

Aton, B., Doukas, A. G., Callender, R. H., Becher, B., & Ebrey, T. G. (1977) *Biochemistry 16*, 2995.

Aton, B., Doukas, A. G., Callender, R. H., Becher, B., & Ebrey, T. G. (1979) *Biochim. Biophys. Acta 576*, 424.

Aton, B., Doukas, A. G., Narva, D., Callender, R. H., Dinur, U., & Honig, B. (1980) *Biophys. J. 29*, 79.

Bagley, K., Dollinger, G., Eisenstein, L., Singh, A. K., & Zimanyi, L. (1982) *Proc. Natl. Acad. Sci. U.S.A. 79*, 4972.

Birge, R. R. (1981) *Annu. Rev. Biophys. Bioeng. 10*, 315.

Braiman, M. (1983) Ph.D. Thesis, University of California, Berkeley, CA.

Braiman, M., & Mathies, R. (1980) *Biochemistry 19*, 5421.

Braiman, M., & Mathies, R. (1982) *Proc. Natl. Acad. Sci. U.S.A. 79*, 403.

Curry, B. (1983) Ph.D. Thesis, University of California, Berkeley, CA.

Curry, B., Broek, A., Lugtenburg, J., & Mathies, R. (1982) *J. Am. Chem. Soc. 104*, 5274.

Curry, B., Palings, I., Broek, A., Pardoen, J. A., Mulder, P. P. J., Lugtenburg, J., & Mathies, R. (1984) *J. Phys. Chem.* (in press).

Eyring, G., Curry, B., Mathies, R., Fransen, R., Palings, I., & Lugtenburg, J. (1980) *Biochemistry 19*, 2410.

Eyring, G., Curry, B., Broek, A., Lugtenburg, J., & Mathies, R. (1982) *Biochemistry 21*, 384.

Lewis, A., Spoonhower, J., Bogomolni, R., Lozier, R., & Stoeckenius, W. (1974) *Proc. Natl. Acad. Sci. U.S.A. 71*, 4462.

Lozier, R., Bogomolni, R., & Stoeckenius, W. (1975) *Biophys. J. 15*, 955.

Maentele, W., Siebert, F., & Kreutz, W. (1981) *FEBS Lett. 128*, 249.

Marcus, M. A., & Lewis, A. (1978) *Biochemistry 17*, 4722.

Mathies, R. (1979) *Chem. Biochem. Appl. Lasers 4*, 55.

Mathies, R., Oseroff, A., & Stryer, L. (1976) *Proc. Natl. Acad. Sci. U.S.A. 73*, 1.

Mathies, R., Freedman, T. B., & Stryer, L. (1977) *J. Mol. Biol. 109*, 367.

Mukohata, Y., Sugiyama, Y., Kaji, Y., Usukura, J., & Yamada, E. (1981) *Photochem. Photobiol. 33*, 593.

Nagle, J., Parodi, L., & Lozier, R. (1982) *Biophys. J. 38*, 161.

Nakanishi, K., Balogh-Nair, V., Arnaboldi, M., Tsujimoto, K., & Honig, B. (1980) *J. Am. Chem. Soc. 102*, 7945.

Oesterhelt, D., & Stoeckenius, W. (1974) *Methods Enzymol. 31*, 667.

Pettei, M. J., Yudd, A. P., Nakanishi, K., Henselman, R., & Stoeckenius, W. (1977) *Biochemistry 16*, 1955.

Potts, W. J., & Nyquist, R. A. (1959) *Spectrochim. Acta 15*, 679.

Rothschild, K. J., & Marrero, H. (1982) *Proc. Natl. Acad. Sci. U.S.A. 79*, 4045.

Smith, S. O., Braiman, M., & Mathies, R. (1983) in *Time-Resolved Vibrational Spectroscopy* (Atkinson, G. H., Ed.) p 219, Academic Press, New York.

Sperling, W., Carl, P., Rafferty, C. N., & Dencher, N. (1977) *Biophys. Struct. Mech. 3*, 79.

Stockburger, M., Klusmann, W., Gattermann, H., Massig, G., & Peters, R. (1979) *Biochemistry 18*, 4886.

Stoeckenius, W., & Bogomolni, R. A. (1982) *Annu. Rev. Biochem. 51*, 587.

Terner, J., Hsieh, C.-L., Burns, A. R., & El-Sayed, M. A. (1979a) *Biochemistry 18*, 3629.

Terner, J., Hsieh, C.-L., & El-Sayed, M. A. (1979b) *Biophys. J. 26*, 527.

Tsuda, M., Glaccum, M., Nelson, B., & Ebrey, T. G. (1980) *Nature (London) 287*, 351.

Warshel, A., & Barboy, N. (1982) *J. Am. Chem. Soc. 104*, 1469.